The Plant Cell, Vol. 12, 949–961, June 2000, www.plantcell.org © 2000 American Society of Plant Physiologists

Developmental Regulation of Methyl Benzoate Biosynthesis and Emission in Snapdragon Flowers

Natalia Dudareva,[a,1] Lisa M. Murfitt,[a] Craig J. Mann,[b] Nina Gorenstein,[a] Natalia Kolosova,[a] Christine M. Kish,[a] Connie Bonham,[b] and Karl Wood[c]

[a] Department of Horticulture and Landscape Architecture, Purdue University, West Lafayette, Indiana 47907
[b] Department of Biochemistry, Purdue University, West Lafayette, Indiana 47907
[c] Department of Chemistry, Purdue University, West Lafayette, Indiana 47907

In snapdragon flowers, the volatile ester methyl benzoate is the most abundant scent compound. It is synthesized by and emitted from only the upper and lower lobes of petals, where pollinators (bumblebees) come in contact with the flower. Emission of methyl benzoate occurs in a rhythmic manner, with maximum emission during the day, which correlates with pollinator activity. A novel *S*-adenosyl-L-methionine:benzoic acid carboxyl methyl transferase (BAMT), the final enzyme in the biosynthesis of methyl benzoate, and its corresponding cDNA have been isolated and characterized. The complete amino acid sequence of the BAMT protein has only low levels of sequence similarity to other previously characterized proteins, including plant *O*-methyl transferases. During the life span of the flower, the levels of methyl benzoate emission, BAMT activity, *BAMT* gene expression, and the amounts of BAMT protein and benzoic acid are developmentally and differentially regulated. Linear regression analysis revealed that production of methyl benzoate is regulated by the amount of benzoic acid and the amount of BAMT protein, which in turn is regulated at the transcriptional level.

INTRODUCTION

Floral scent is a key modulating factor in plant–insect interactions and plays a central role in successful pollination, and thus in fruit development, of many crop species. Flower fragrances vary widely among species in terms of the number, identity, and relative amounts of constituent volatile compounds (Knudsen and Tollsten, 1993; Knudsen et al., 1993). Closely related plant species, which rely on different insects for pollination, produce different odors (Henderson, 1986; Raguso and Pichersky, 1995). Often, characteristic floral odors are correlated with the type of pollinators. Species pollinated by bees and flies tend to have scents that are defined (by humans) as sweet, whereas those pollinated by beetles have musty, spicy, or fruity odors (Dobson, 1994).

Many volatile components of flowers have been identified; however, the mechanism of flower fragrance formation is not well understood. Recent investigations of floral scent production in *Clarkia breweri* are the first examples of the isolation of enzymes and genes responsible for the biosynthesis of scent volatiles. The enzymes *S*-linalool synthase, *S*-adenosyl-L-methionine (SAM):(iso)eugenol *O*-methyl transferase, acetyl-CoA:benzyl alcohol acetyltransferase, and SAM:salicylic acid carboxyl methyl transferase, which catalyze the formation of linalool, methyl(iso)eugenol, benzylacetate, and methyl salicylate, respectively, and their corresponding genes have been isolated and characterized (Pichersky et al., 1994, 1995; Dudareva et al., 1996, 1998a, 1998b; Wang et al., 1997; Wang and Pichersky, 1998; Ross et al., 1999; reviewed in Dudareva and Pichersky, 2000). It has been shown that in *C. breweri*, flowers synthesize their scent compounds de novo in the tissues from which they are emitted, and the emission levels, corresponding enzyme activities, and amounts of mRNA are all spatially and temporally correlated. In general, the expression of these genes is greatest in petals just before anthesis and is restricted to the epidermal cell layer of floral tissues.

Although production of volatile scent compounds appears to be widespread in the plant kingdom, information about their de novo biosynthesis (as distinct from their possible release from glucosides; see Oka et al., 1999) and about regulation of the genes involved is limited and based to date on analysis of a single model system, moth-pollinated *C. breweri*. Whether similar molecular mechanisms are involved in regulation of floral scent production in other plant species is currently unclear. We have begun to address this question by studying bee-pollinated snapdragon flowers (Scrophulariaceae). The snapdragon model has several important advantages over the *C. breweri* system: a well-developed

[1] To whom correspondence should be addressed. E-mail dudareva@hort.purdue.edu; fax 765-494-0391.

genetic map (Stubbe, 1966), a transposon gene cloning system (Martin et al., 1990), an available transformation protocol (Heidmann et al., 1998), and rhythmic emission (see below). Several genes encoding flower pigment biosynthetic enzymes and genes controlling flower development have been isolated from snapdragon (Coen et al., 1986; Sommer and Saedler, 1986; Coen and Meyerowitz, 1991; Irish and Yamamoto, 1995), but no information about enzymes and genes involved in the synthesis of flower scent compounds has been published.

In this study, we present a detailed analysis of the production of a volatile ester, methyl benzoate, in snapdragon flowers. We show that methyl benzoate is produced by enzymatic methylation of benzoic acid in the reaction catalyzed by SAM:benzoic acid carboxyl methyl transferase (BAMT). During the life span of the flower, the levels of methyl benzoate emission, BAMT activity, *BAMT* gene expression, the BAMT protein, and benzoic acid are developmentally and differentially regulated. Our results provide evidence that production of methyl benzoate is regulated by the amount of benzoic acid and the amount of the BAMT protein, which in turn is regulated at the transcriptional level. Overall, the data suggest that similar molecular mechanisms may be involved in the regulation of floral scent production in different plant species.

RESULTS

Detection of Volatiles Emitted by Intact Flowers and Temporal and Rhythmic Variations in Emission of the Major Component, Methyl Benzoate

Headspace analysis in combination with gas chromatography–mass spectrometry (GC-MS) of volatiles emitted from flowers of 37 different Antirrhinum cultivars revealed that snapdragon flower scent is dominated by myrcene, *trans*-β-ocimene, and methyl benzoate. Methyl benzoate is the most abundant scent compound detected in the majority of snapdragon varieties. In these experiments, we collected headspace compounds from a single inflorescence with eight to 12 flowers at 24-hr intervals. No correlation was found between fragrance composition and flower color. The greatest amount of methyl benzoate emission was found in the Maryland True Pink cultivar, where it accounts for ~60% of the total volatiles (Table 1). This cultivar was used for further investigations.

To determine variations in emission of methyl benzoate during the life span of flower development, we conducted time-course headspace collections from single, living flowers at 24-hr intervals. Unopened flowers (buds) emitted no methyl benzoate (Figure 1A). Emission of methyl benzoate began at anthesis but at a very low level (1.8 μg per flower for 24 hr), reached a peak between days 5 to 8, and declined thereafter. At peak, 56.5 μg was emitted per flower in 24 hr.

Table 1. Major Volatile Compounds Identified from Maryland True Pink Snapdragon Flowers

Compound	Volatile Production[a] (μg/flower/24 hr)	Relative Amount (%)[b]
Myrcene	7.7 ± 2.1	8.1
trans-β-ocimene	26.0 ± 5.9	27.4
Methyl benzoate	56.5 ± 7.3	59.5

[a] Production of volatile compounds is shown for 5-day-old flowers.
[b] Minor volatile compounds comprise ~5% of total volatile production.

To determine variations in methyl benzoate emission during a 24-hr period, we collected volatile compounds from a 3-day-old flower during a 12-hr light period and a 12-hr dark period. These results revealed that snapdragon flowers produce methyl benzoate in a rhythmical, diurnal manner. Floral odor collected during the daytime contained four times more methyl benzoate per flower than that collected during the night. We also performed headspace collections at 3-hr intervals during the light period and at 6-hr intervals at night to check for possible fluctuations in methyl benzoate emission during the light period (Figure 1B). The emission of methyl benzoate was not stable during the day but peaked between 9 AM and 4 PM. Maximum emission of methyl benzoate correlated with the light intensity in the greenhouse (Figure 1B).

Analysis of BAMT Activity in Floral Tissues and at Different Stages of Flower Development

Although methyl benzoate has been reported in the floral scent of >30 different species (Knudsen et al., 1993), the immediate biochemical step leading to its synthesis has not previously been elucidated. It seemed likely, however, that methyl benzoate could be synthesized by enzymatic methylation of benzoic acid with SAM as the methyl group donor, in a reaction analogous to the synthesis of methyl salicylate from SAM and salicylic acid (Dudareva et al., 1998b). Therefore, we devised an enzymatic assay to test for BAMT activity using nonradioactive benzoic acid and ^{14}C-SAM as the methyl donor (Figure 2).

Using this assay, we analyzed BAMT activity in crude extracts from different parts of snapdragon flowers and at different stages of flower development. The stages ranged from just before anthesis, when mature flower buds appear, to 12 days after anthesis. Antirrhinum flowers are zygomorphic; they contain five small sepals and five petals fused at the base into a tube that divides distally into the upper and lower lobes. The two upper and three lower lobes close the mouth of the corolla tube (Coen and Meyerowitz, 1991; Figures 3A and 3B). Crude extracts were prepared from different flower organs and also from different regions of the

corolla (the upper petal lobes, the lower petal lobes, and the tube) of 6-day-old flowers and tested for BAMT activity.

The majority of BAMT activity was found in the upper and lower lobes, with much less activity in the tube and anthers (Figure 3C). BAMT activity, calculated per milligram of fresh weight of tissue, was ~10-fold higher in lower and upper lobes than in the tube (4.07, 2.8, and 0.37 pkat mg^{-1} fresh weight, respectively). None of the remaining floral organs (pistils, sepals, and ovaries) or leaves was found to contain BAMT activity. These results suggest that the main sites of methyl benzoate synthesis are the upper and lower petal lobes, which make almost equal contributions to the whole-flower fragrance.

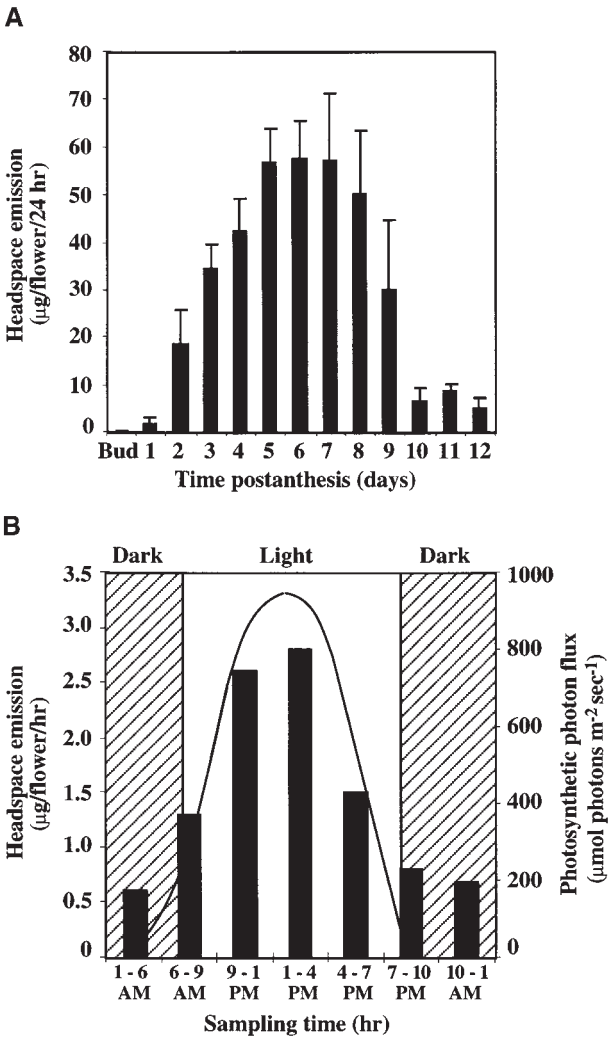

Figure 1. Emission of Methyl Benzoate from Snapdragon Flowers Measured by Headspace Collection and GC-MS Analysis.

(A) Emission of methyl benzoate during the life span of the flower, from mature flower buds 1 day before opening to 12 days after anthesis. Data are means ±SE ($n = 5$).

(B) Emission of methyl benzoate within a 24-hr period. Headspace collections were performed at 3-hr intervals during the light period and at 6-hr intervals at night. Black bars show emission; the curved line shows photosynthetic photon flux.

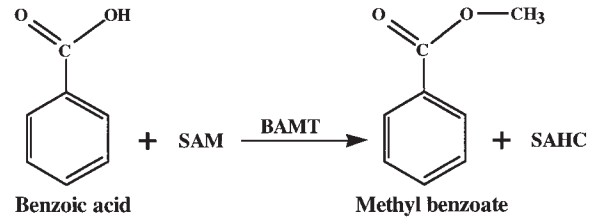

Figure 2. Reaction Catalyzed by BAMT.

SAM is a donor of the methyl group; SAHC, *S*-adenosyl-L-homocysteine.

We also found that the level of BAMT activity in petals is developmentally regulated. The total BAMT activity gradually increased during the first 5 days after anthesis, remained relatively stable during the next 5 days, and decreased thereafter (Figure 3D). No BAMT activity was detectable in flower buds 1 day before the opening of the flower.

Purification of BAMT and Isolation and Characterization of BAMT cDNA Clones

The BAMT protein was successively purified from 5- to 10-day-old upper and lower petal lobes (floral tissue with the highest BAMT-specific activity) by DE53 anion exchange, phenyl–Sepharose 6FF, and MonoQ chromatography. After the MonoQ chromatography step, the fraction with the most BAMT activity was determined on an SDS–polyacrylamide gel to contain one major protein, with an apparent molecular mass of 49 kD. This protein was also tested with several other naturally occurring substrates such as salicylic acid and *trans*-cinnamic acid and their derivatives (3-hydroxybenzoic acid, 4-hydroxybenzoic acid, benzyl alcohol, and 2-coumaric, 3-coumaric, and 4-coumaric acids). When these compounds were added to this protein, no activity was detected.

Sequencing the N terminus of the 49-kD protein was unsuccessful because of a blocked N terminus. Therefore, we subjected the purified BAMT protein to lysyl endopeptidase cleavage and determined the amino acid sequences from the six internal regions. Two peptide sequences of 25 and 12 residues were used to construct degenerate oligonucleotides for polymerase chain reaction (PCR) amplification of a 450-nucleotide fragment of the BAMT coding region (see Methods). The amplified fragment, in turn, was used to isolate cDNAs from a petal-specific Anthirrinum cDNA library. Several cDNA clones, all containing the same open reading

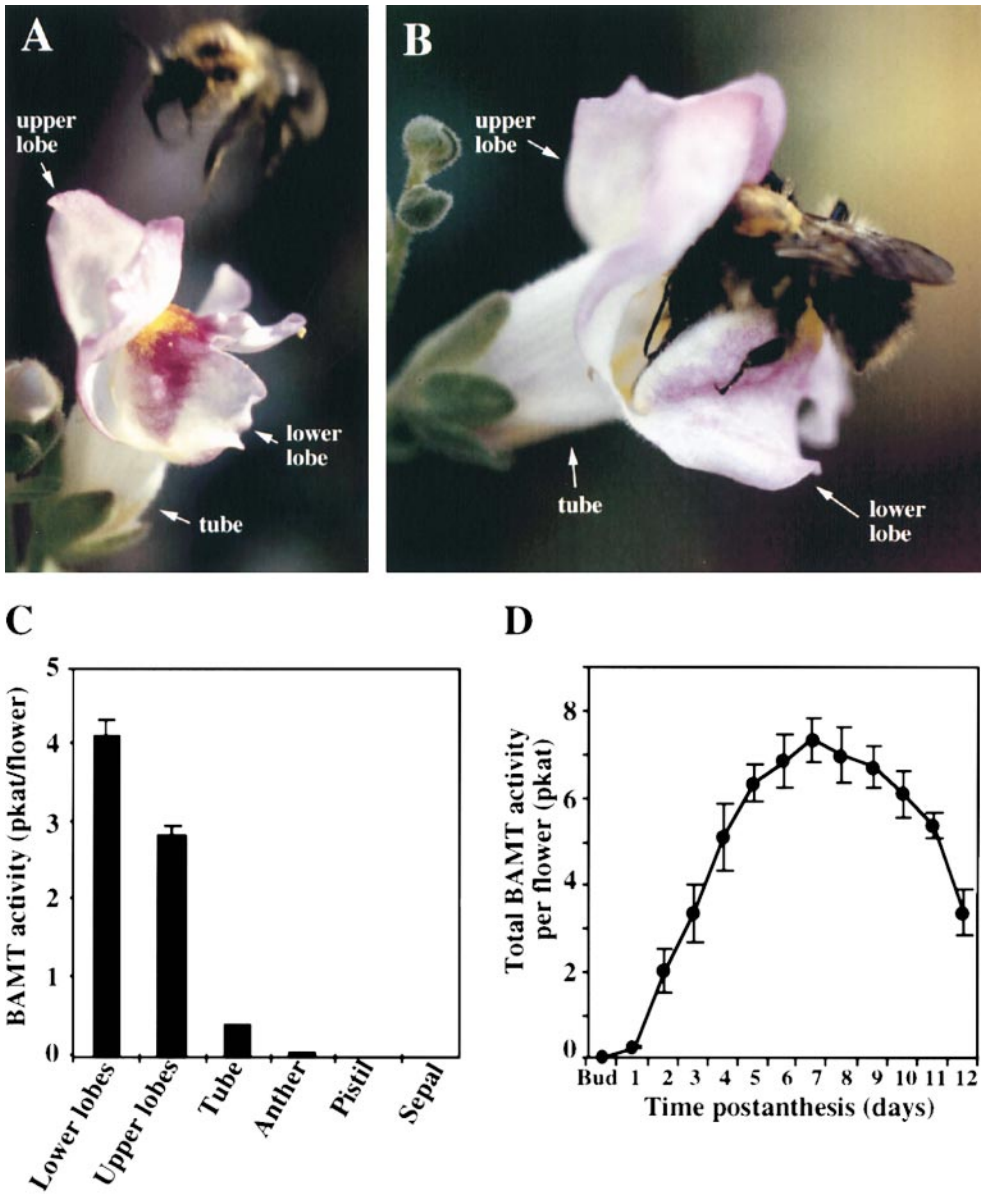

Figure 3. Amounts of BAMT Activity in Different Parts of a Snapdragon Flower and at Different Stages of Flower Development.

(A) Antirrhinum flower with a visiting bumblebee. The bumblebee is in flight, approaching the flower. Only the upper and lower petal lobes are facing the bee during landing.

(B) The bumblebee is entering the snapdragon flower in the classic way. The bee opens the mouth of the corolla tube, and only upper and lower lobes of the petals come in contact with the bee's body. In this way, a bee can be perfumed by floral scent produced only in the upper and lower petal lobes. Photographs **(A)** and **(B)** have been donated by Iris Heidmann from the Max-Planck-Institut für Züchtungsforschung, Cologne, Germany.

(C) BAMT activity in different flower parts of a 6-day-old snapdragon flower. The values of 120, 130, and 200 mg were used for the total weight of the upper and lower lobes and the tube, respectively. Protein concentrations for the upper and lower lobes and the tube were 1.45, 1.83, and 0.72 mg mL^{-1}, respectively, and can be used to calculate specific activities per milligram of protein. Values are the average of five independent measurements. Error bars indicate standard deviations.

(D) Changes in BAMT activity during flower development. Data are shown only for upper and lower petal lobes that contained BAMT activity. For each time point, enzyme assays were run in duplicate on at least five independent crude extract preparations, and the standard deviations were obtained.

frame of 364 codons (starting with a methionine codon), were isolated and sequenced. The protein encoded by these cDNAs contained all six peptide sequences determined experimentally.

The sequence of the BAMT protein does not contain the consensus motifs found in many plant SAM-dependent *O*-methyl transferases (Ibrahim, 1997; Ibrahim et al., 1998; Joshi and Chiang, 1998). However, the predicted amino acid sequence of the BAMT protein is ~40% identical to salicylic acid carboxyl methyl transferase recently isolated from *C. breweri* (Ross et al., 1999; Figure 4). These enzymes thus define a new class of plant carboxyl methyl transferases. They share the ability to transfer the methyl group of SAM to a free carboxyl group.

Database searches revealed sequences for eight unidentified proteins with 20 to 40% identity to BAMT. All of these sequences are encoded by Arabidopsis genes and are predicted to contain 360 to 370 amino acid residues. These proteins may all belong to a class of carboxyl methyl transferases with different substrate specificities. The sequences of two hypothetical proteins with the highest identity to BAMT are also shown in Figure 4. In addition, there are a number of expressed sequence tags in the databases with similarity to BAMT.

Functional Expression of BAMT cDNA in *Escherichia coli*

To verify that the isolated cDNA clone encoded BAMT, we expressed the protein in *E. coli*. When cell lysates were tested with benzoic acid, salicylic acid, cinnamic acid, and their derivatives, high activity (7.53 pkat mg^{-1} protein) was detected with benzoic acid as substrate but no activity with any of the others. Moreover, the culture medium of the *E. coli* cells expressing BAMT contained a small amount of methyl benzoate (0.1 $\mu g\ mL^{-1}$; Figures 5A and 5C). The amount of methyl benzoate in the medium increased to 0.66 $\mu g\ mL^{-1}$ when the growing medium was supplemented with 5 $\mu g\ mL^{-1}$ benzoic acid (Figures 5A and 5D). *E. coli* cells that contained a pET-T7 (11a) plasmid without the BAMT coding region did not have any detectable BAMT activity and did not produce methyl benzoate (Figure 5B).

Tissue- and Developmental Stage–Specific BAMT Expression

RNA gel blot analysis was used to determine the tissue specificity of *BAMT* gene expression. The highest amounts of *BAMT* mRNA were observed in the upper and lower lobes of petals (Figure 6A). A small amount of *BAMT* transcripts was also detected in the tube. No detectable signals were found in pistils, stamens, sepals, or leaf tissue. Because BAMT activity and *BAMT* mRNA were found mostly in upper and lower lobes of petals, we examined the steady state levels of *BAMT* mRNA in Maryland True Pink petals during flower development. *BAMT* mRNA was first detected in 1-day-old flowers and increased until peaking on day 4 after anthesis (Figures 6B and 6C). By day 6 after anthesis, mRNA level had declined 30% from the peak value, remained relatively stable until day 9, and decreased thereafter.

The amounts of BAMT protein in upper and lower petal lobes of snapdragon flowers over the developmental period from mature buds to day 12 after anthesis were determined quantitatively by using the chemiluminescence protein gel blotting technique. The polyclonal anti–BAMT antibodies, raised against the denatured BAMT protein overexpressed in *E. coli*, selectively recognized one protein with an apparent molecular mass of 49 kD in crude petal extracts separated by SDS-PAGE. The BAMT protein was first detected in 2-day-old flowers, indicating a very low amount of this protein in younger flowers (Figure 7A). Unlike the level of mRNA, the level of BAMT protein was greatest on day 7 after anthesis (Figure 7B).

Accumulation of Benzoic Acid in Petal Tissue of Snapdragon Flowers

Because BAMT catalyzes the final step in the biosynthesis of methyl benzoate, regulation of the production of methyl benzoate may also occur at earlier biochemical steps in the pathway. To test this hypothesis, we measured the endogenous pools of benzoic acid in petal tissue during flower development. A substantial endogenous pool of benzoic acid was found in petal tissue (upper and lower lobes), and the size of this pool changed during development (Figure 8). The highest content of benzoic acid was found on day 2 after anthesis (19.6 $\mu g\ g^{-1}$ fresh weight; Figure 8A), when the emission of methyl benzoate and the activity of BAMT are relatively low (~30% of maximum; Figures 1A and 3D). The petal concentration of benzoic acid declined in a way that coincided with the increasing amounts of BAMT activity and emission of methyl benzoate until day 8 after anthesis. After that time, the amount of benzoic acid continued to decrease, whereas the amount of BAMT activity remained relatively high (Figures 3D and 8A). Thus, the low emission of methyl benzoate in older flowers (Figure 1A) could be due to the limited amount of benzoic acid.

DISCUSSION

Temporal and Rhythmic Variations in Methyl Benzoate Emission

Flowers of many plant species attract pollinators by producing different complex mixtures of volatile compounds that give each species unique, characteristic fragrances. Volatile compounds emitted from flowers play a prominent role in the localization and selection of flowers by insects (Dobson,

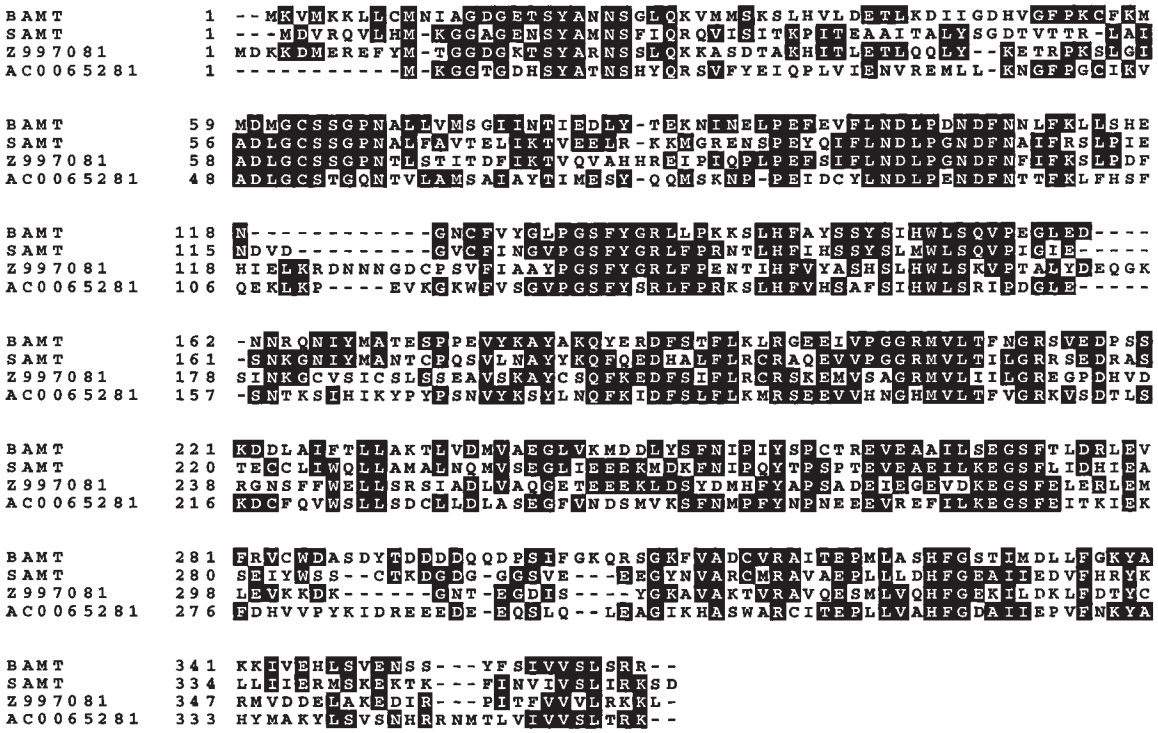

Figure 4. Comparison of the Predicted Amino Acid Sequence of Snapdragon BAMT Protein with Related Proteins.

SAMT is SAM:salicylic acid carboxyl methyl transferase from *C. breweri* (GenBank accession number AF133053). Proteins with GenBank accession numbers Z997081 and AC0065281 correspond to two hypothetical proteins from Arabidopsis. Black boxes indicate conserved amino acid residues, and dashes indicate gaps that have been inserted for optimal alignment. Sequences were aligned and displayed using the ClustalW and Boxshade 3.21 software programs (Human Genome Sequencing Center, Houston, TX).

1994). Although very little is known about the effect of individual scent volatiles on insect–flower interactions, measurements of the electroantennogram responses of insects have shown that aromatic esters are important floral attractants (Henning and Teuber, 1992; Raguso et al., 1996; Raguso and Light, 1998).

Our results show that newly opened young flowers, which are not ready to function as pollen donors because their anthers have not yet dehisced, produce fewer odors and are less attractive to pollinators than are older flowers (Figure 1A). A recent investigation of the frequency and duration of bumblebee visits to snapdragon flowers revealed that 1- and 2-day-old flowers received fewer and shorter visits than did 4-day-old and older flowers (Jones et al., 1998).

Although many plants emit volatile compounds continuously and at a constant level during flowering, other flowering plants emit scent in a rhythmic manner with a diurnal or nocturnal maximum (Matile and Altenburger, 1988; Loughrin et al., 1990; Nielsen et al., 1995; Helsper et al., 1998). The rhythmic release of volatiles from some flowers is often correlated with the corresponding temporal activity of their known pollinators (Loughrin et al., 1990; Schiestl et al., 1997). Because snapdragon flowers are pollinated by bumblebees during the daytime, we expected flowers to emit fewer volatiles during the night than during the day. In fact, the amount of methyl benzoate released per hour by a single snapdragon flower was four times higher during the daytime than at night (Figure 1B). Emission of methyl benzoate follows diurnal cycles, with the highest emission rate between 9 AM and 4 PM (Figure 1B), and coincides with peak foraging activity of bumblebees (Heinrich, 1979).

Biosynthesis of Methyl Benzoate in Floral Tissues and at Different Stages of Flower Development

The total activity of BAMT, the final enzyme in the biosynthesis of the volatile ester methyl benzoate, was greatest in the upper and lower lobes of the petals, suggesting that these parts are primarily responsible for the production and emission of methyl benzoate (Figure 3C). In flowers of many plant species, the petals are the principal emitters of volatiles (Dobson, 1994; Dudareva et al., 1999). By further dissecting the snapdragon petals, we showed that production

of floral volatiles in snapdragon flower was even more restricted, limited mostly to the upper and lower lobes of the petals. In flowers such as snapdragon, pollinators must open the petals after landing to gain access to the nectar. The upper and lower lobes of the petals come into contact with the bee's body during landing (Figures 3A and 3B), enabling the bee to accumulate floral scent molecules on its body surface. This floral scent is then carried to the nest and can, in turn, help the bee to recruit new foragers to locate the flowers. The recruitment rate can be increased by intensifying the odor at a food source (Von Frisch, 1971).

We have also found that the level of BAMT activity in upper and lower petal lobes is developmentally regulated. Total BAMT activity gradually increased during the first 5 days after anthesis, as did the emission of methyl benzoate (Figures 1A and 3D). It remained relatively stable during the next 5 days, although the emission of methyl benzoate declined, and decreased thereafter. In *C. breweri* flowers, the activities of four enzymes involved in floral scent production were found (Dudareva and Pichersky, 2000) to follow two different developmental patterns. The activities of two enzymes, *S*-linalool synthase and SAM:salicylic acid carboxyl methyl transferase, increased in young flowers and, although they declined in older (5-day-old) flowers, remained relatively high (40 to 50% of the maximum level), even though emission of linalool and methyl salicylate had practically ceased. The activities of two other enzymes, SAM:(iso)eugenol *O*-methyl transferase and acetyl-CoA:benzyl alcohol acetyltransferase, showed $\leqslant$10% decline at the end of the life span of the flower, although emissions of corresponding volatile compounds declined substantially (Dudareva and Pichersky, 2000). The BAMT enzyme from snapdragon flowers appears to belong to the first group, because its activity declined at the end of the life span of the flower (9 to 12 days after anthesis) to 46% of the maximum level, without the concomitant emission of methyl benzoate (Figures 1A and 3D).

Regulation of Methyl Benzoate Emission in Snapdragon Flowers

Recent progress in our understanding of floral scent production in plants, based so far only on *C. breweri* as the model system, has indicated that scent compounds are synthesized de novo in epidermal cells of the floral organs from which they are emitted (primarily the petals). The amounts of activity of the enzymes involved in scent production and, indirectly, in scent emission are regulated mainly at the transcriptional levels at the site of emission (Dudareva et al., 1996, 1998a; Wang et al., 1997). Our results demonstrate that, considering the different parts of snapdragon flower, the upper and lower lobes of petals contain the majority of *BAMT* transcripts (Figure 6A). These mRNA contents correlate strongly with the BAMT activity profile (Figure 3C), that is, high enzyme activity only in petals and very low or no activity in other floral organs and leaves. The steady state levels of *BAMT* mRNA in petals are developmentally regulated, being greatest on day 4 after anthesis (Figures 6B and 6C). The amounts of methyl benzoate emission, BAMT activity, and mRNA in petals all rise and fall simultaneously until the end of the life span of the flower, with mRNA values peaking 1 day ahead of enzyme activity and emission (Figures 1A, 3D, and 6C). A positive correlation between amounts of emission, enzyme activity, and mRNA indicates that, similar to *C. breweri*, BAMT enzyme activity is regulated primarily at a pretranslational level. When plotting BAMT activity at different stages of flower development against the amount of protein in those stages, linear regression analysis revealed a correlation coefficient of 0.98 (Figure 9A). Such a strong correlation between enzyme activity and protein provides compelling evidence that differences in BAMT activity at different stages of development are the result of changes in the abundance of BAMT protein rather than post-translational modification. These results suggest that, similar to *C. breweri*, the activities of scent biosynthetic enzymes in snapdragon are regulated by transcription of the corresponding genes in the flower.

Because BAMT is the final enzyme in the biosynthesis of methyl benzoate (Figure 2), the regulation of methyl benzoate production could also occur at earlier biochemical steps in the pathway by controlling the supply of the substrate, benzoic acid. Data presented in this study show that the sizes of the benzoic acid pools in upper and lower petal lobes are indeed developmentally regulated (Figure 8A). The low amount of benzoic acid in old flower petals (9 to 12 days after anthesis) may indicate that the earlier biochemical steps in the pathway are blocked as the flower ages or that synthesized benzoic acid is required for some other processes in the cells. Plotting the emission of methyl benzoate from snapdragon flowers against predicted production of methyl benzoate (Figure 9B; see Methods for details) gives a correlation coefficient for linear regression analysis of 0.95, indicating that production of methyl benzoate is regulated by the amount of benzoic acid and the amount of BAMT protein, with the latter being regulated at the transcriptional level.

We found that emission of methyl benzoate declines toward the end of the life span of the flower (9 to 12 days after anthesis; Figure 1A), whereas BAMT activity remains relatively high (46% of the maximum level; Figure 3D). Interestingly, BAMT activity in 3- and 12-day-old flowers is similar (3.4 pkat per flower; Figure 3D), indicating that the protein in old flowers is capable of producing the same amount of methyl benzoate as that of 3-day-old flowers. However, the amount of ester emission is almost seven times higher in young flowers than in old ones (Figure 1A). The finding that the amount of benzoic acid in petal tissue of 12-day-old flowers is only one-fifth that of 3-day-old flowers (Figure 8A) indicates that the amount of substrate present is a limiting factor.

High levels of activity of biosynthetic enzymes in old flowers without concomitant emission of volatile products were

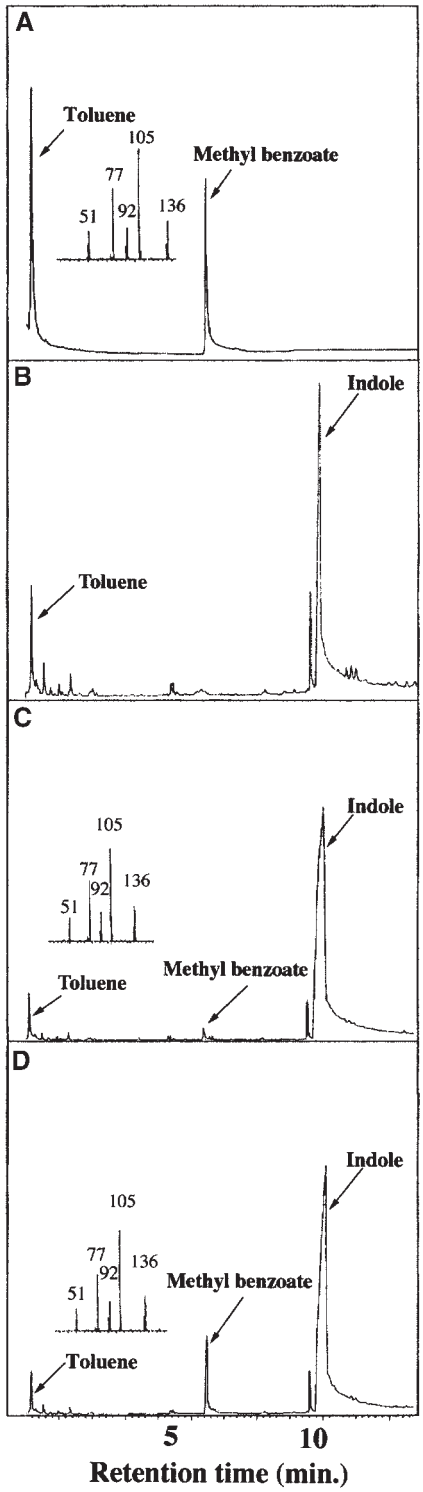

Figure 5. Detection of Methyl Benzoate in the Medium of *E. coli* Cells Expressing Snapdragon BAMT.

(A) GC-MS analysis of methyl benzoate standard.
(B) Analysis of the medium of *E. coli* cells expressing pET-T7 (11a) vector with no insert after induction with isopropyl-β-D-thiogalactopyranoside.
(C) Analysis of the medium of *E. coli* cells expressing snapdragon BAMT after induction with isopropyl-β-D-thiogalactopyranoside. The growing medium was not supplemented with benzoic acid. The mass spectrum is that of the peak eluted at the same retention time as the authentic methyl benzoate standard **(A)**.
(D) Analysis of the medium of *E. coli* cells expressing snapdragon BAMT after induction with isopropyl-β-D-thiogalactopyranoside. The growth medium was supplemented with 5 μg mL^{-1} benzoic acid. The mass spectrum is that of the peak eluted at the same retention time as the authentic methyl benzoate standard **(A)**.
Toluene was added to all samples as an internal standard. Indole is produced by all *E. coli* cells (Dudareva et al., 1998a; Ross et al., 1999). Numbered peaks in **(A)**, **(C)**, and **(D)** represent mass-to-charge ratios of molecular ion and fragment ions of methyl benzoate.

also found in *C. breweri* (Pichersky et al., 1994; Wang et al., 1997; Dudareva et al., 1998b); however, the pools of available substrates were not determined in those cases. Our current data show that the total amount of substrate in the cell is involved in regulation of biosynthesis and emission of flower volatiles and that the low emission of methyl benzoate in old flowers is the result of low amounts of benzoic acid in petal tissue (Figures 8A and 9B) (it is possible, of course, that the amount of SAM also is low at the end of the flower's life).

Overall, our results with snapdragon flowers, together with the data obtained in *C. breweri*, suggest that common regulatory mechanisms are involved in floral scent production in different plant species. This study contributes additional evidence that in both *C. breweri* and snapdragon flowers, scent compounds are produced de novo in the tissues from which they are emitted. Because the amount of benzoic acid present is involved in the regulation of methyl benzoate production and emission, it would be of interest to examine whether it is also responsible for the rhythmic emission of volatile ester.

METHODS

Plant Material, Headspace Collection, and Gas Chromatography–Mass Spectrometry Analysis

Seeds of 37 different Antirrhinum cultivars were kindly provided by Ball Seed Co. (West Chicago, IL). Plants were grown under standard greenhouse conditions. Volatiles emitted from snapdragon flowers were determined by headspace analysis, as described previously (Raguso and Pichersky, 1995; Raguso and Pellmyr, 1998). Trapped floral scent compounds were analyzed by gas chromatography–mass spectrometry (GC-MS) with a FinniganMAT GCQ instrument (Thermoquest, San Jose, CA) (injector temperature 230°C, injector volume 1 μL, and split ratio 50:1) using a DB-1 nonpolar capillary column (30 m × 0.25 mm [i.d.]; film thickness 0.25 μm). Ionization en-

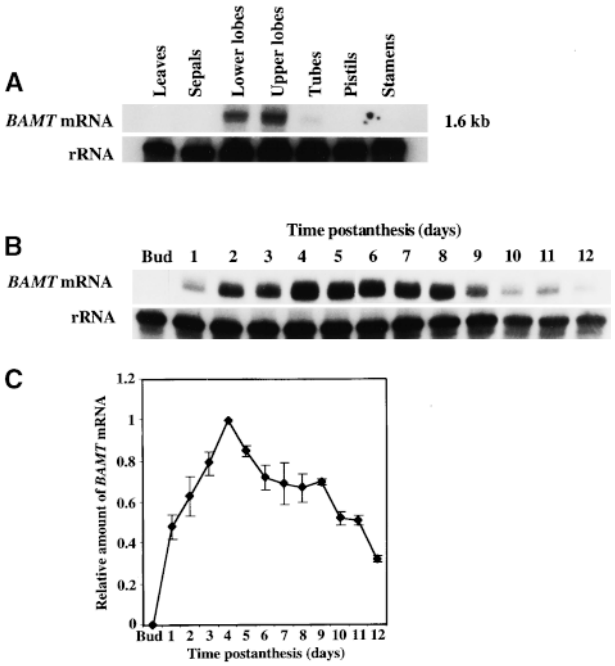

Figure 6. RNA Gel Blot Analysis of *BAMT* Gene Expression.

(A) Tissue specificity of *BAMT* gene expression. Total RNA was isolated from young leaves, sepals, pistil, stamens, upper and lower petal lobes, and tubes of a 6-day-old flower; 7 μg of total RNA was loaded in each lane. The top gel represents the results of hybridization with a *BAMT* probe. The length of the *BAMT* mRNA was estimated as 1.6 kb by comparison with RNA molecular markers in an adjacent lane. Autoradiography was for 24 hr. The blot was rehybridized with an 18S rDNA probe (bottom) to standardize sample results.
(B) Developmental changes in steady state *BAMT* mRNA amounts in upper and lower lobes of snapdragon petals. Shown is RNA gel blot hybridization with mRNA from upper and lower petal lobes at different stages of development. The yield of total RNA from upper and lower petal lobes per gram of tissue (fresh weight) at different stages of development was very similar at all stages, varying from 120 to 190 μg. Each lane contained 3 μg of total RNA. Autoradiography was for 24 hr. The blots were rehybridized with an 18S rDNA probe (bottom) to standardize sample results.
(C) Plot of the variations in *BAMT* mRNA content in upper and lower petal lobes throughout the life span of the flower. Values were obtained by scanning RNA gel blots with a PhosphorImager. Each point is the average of five different experiments (including the one shown in **[B]**), and values were corrected by standardizing for the amounts of 18S rRNA measured in the same runs. Error bars indicate standard deviations.

ergy was set at 70 eV. Column temperature was held at 50°C for 1 min and then heated to 240°C at 10°C min^{-1}. The mass spectrometer was scanned from 41 to 400 amu. Ambient volatiles collected at the same times as the samples were used as controls. Components were first identified from a computer database containing several thousand mass spectra and were confirmed by comparing retention times and mass spectra with those of authentic standards.

S-Adenosyl-L-Methionine:Benzoic Acid Carboxyl Methyl Transferase Enzyme Assays and Product Analysis

Crude protein extracts were prepared by homogenizing freshly excised flower parts in a chilled glass homogenizer in the presence of ice-cold extraction buffer (5:1 [v/w] buffer/tissue) containing 50 mM BisTris-HCl, pH 6.9, 10 mM β-mercaptoethanol, 5 mM $Na_2S_2O_5$, 1% (w/v) polyvinylpyrrolidone (PVP-40), 1 mM phenylmethylsulfonyl fluoride, and 10% (v/v) glycerol. The slurry was centrifuged for 10 min to produce a supernatant containing the enzyme activity. For each collection time, flower parts from at least five flowers from different plants were combined. Total soluble proteins were determined by the Bradford method (Bradford, 1976) using the Bio-Rad (Hercules, CA) protein reagent and BSA as a standard.

Enzyme activity was determined by measuring how much of the ^{14}C-labeled methyl group of *S*-adenosyl-L-methionine (SAM) was transferred to the carboxyl group of benzoic acid. The standard reaction mixture (100 μL) consisted of 20 μL of crude extract (25 to 40 μg of protein) and 100 μM of labeled SAM (containing 0.1 μCi) in assay buffer (50 mM Tris-HCl, pH 7.5, and 3 mM 2-mercaptoethanol) with

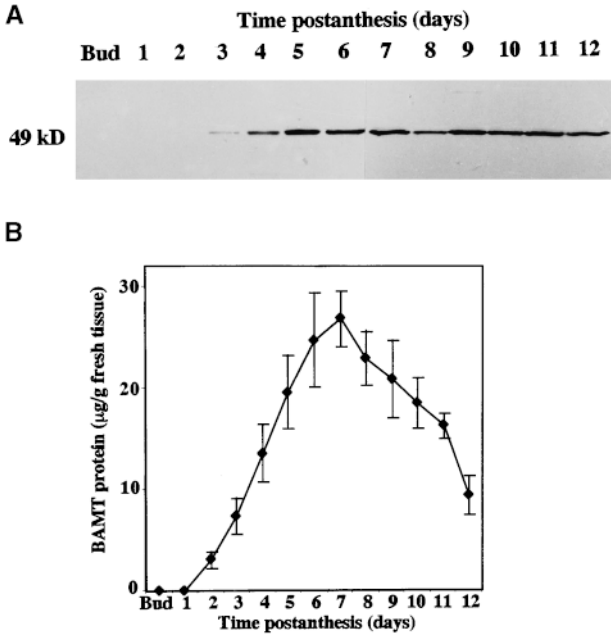

Figure 7. Developmental Changes in BAMT Protein Concentrations in Upper and Lower Lobes of Snapdragon Petals.

(A) Expression of the BAMT protein in upper and lower petal lobes at different stages of development. Representative protein gel blot shows the 49-kD protein recognized by anti–BAMT antibodies. Proteins were extracted from upper and lower petal lobes at different stages of development, and 20 μg of protein was loaded in each lane.
(B) Plot of variations in the amounts of BAMT protein in upper and lower petal lobes throughout the life span of the flower. Values were obtained by scanning the protein gel blots. Each point is the average of seven different experiments (including the one shown in **[A]**). Standard error values are indicated as vertical bars.

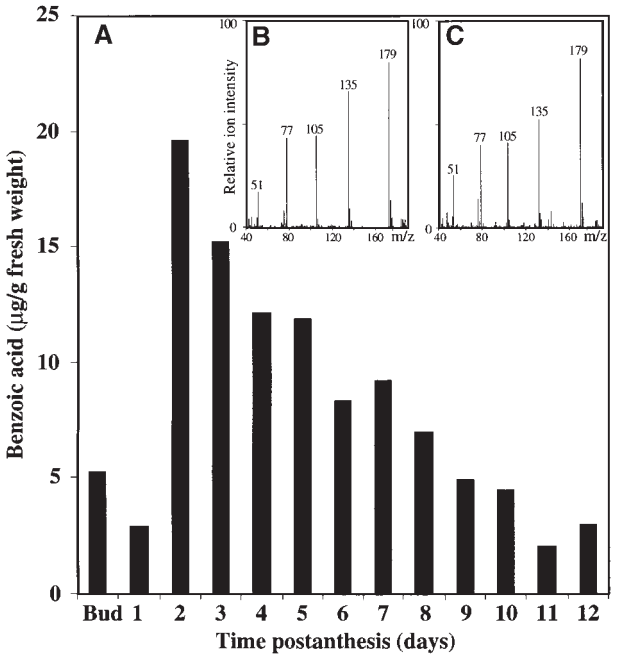

Figure 8. Developmental Changes in the Amount of Benzoic Acid in Upper and Lower Lobes of Snapdragon Petals.

(A) Benzoic acid, extracted from upper and lower petal lobes at different stages of development by supercritical carbon dioxide extraction, was analyzed by HPLC.

(B) Electron impact mass spectrum of derivatized authentic benzoic acid. Molecular weight of derivatized benzoic acid is 194; after ionization, the highest mass-to-charge ratio (*m/z*) is the loss of a CH_3 radical, resulting in an *m/z* of 179.

(C) Electron impact mass spectrum of derivatized benzoic acid isolated from 2-day-old snapdragon petals. A peak corresponding to benzoic acid was collected after HPLC, derivatized, and analyzed by GC-MS.

In **(B)** and **(C)**, the numbered peaks are the *m/z* values for the fragment ions of the derivatized benzoic acid.

2 mM benzoic acid and 0.5 mM EDTA. After incubation for 30 min at 20°C, the radioactively labeled methylated product was extracted by adding 100 μL of hexane, and 50 μL of the organic phase was counted in a liquid scintillation counter (model LS 6800; Beckman, Fullerton, CA). The raw data (counts per minute) were converted to picokatals (picomoles of product produced per second) based on the specific activity of the substrate and efficiency of counting. Controls included assays with boiled protein extracts and without substrate; the background radioactivity measured in such assays was subtracted from all of the results.

Product verification was performed by thin-layer chromatography, as previously described (Wang et al., 1997) and by GC-MS. For GC-MS, the enzymatic reaction was scaled up to 1 mL (final volume) and contained 1 mM nonradioactive SAM (Sigma). The reaction was performed for 1 hr, and product was extracted with 1 mL of hexane, concentrated, and injected into the gas chromatograph–mass spectrometer.

Enzyme Purification and Protein Sequencing

The enzyme activity from upper and lower petal lobes of 5- to 10-day-old snapdragon flowers was purified in a series of chromatographic steps involving a DEAE anion exchange column (DE53; Whatman International, Maidstone, UK), a phenyl–Sepharose 6FF (low sub; phenyl substitution at 20 μmol mL^{-1} gel) column (Pharmacia Biotech, Piscataway, NJ), and another anion exchange column, MonoQ, on Pharmacia's fast performance liquid chromatography system. A complete description of the purification protocol will be presented elsewhere (L.M. Murfitt, C.J. Mann, and N. Dudareva, unpublished data). Sequence analysis was performed with peptides produced by lysyl endopeptidase (Wako BioProducts, Richmond, VA) cleavage of purified benzoic acid carboxyl methyl transferase (BAMT) protein. The digestion products were separated on a narrow-bore HPLC, using a C_{18} (21 × 250 mm) reversed-phase column, and the amino acid sequences from six internal regions were determined in a protein sequencer (model Procise 491; Applied Biosystems, Foster City, CA) by using standard protocols.

cDNA Library Construction

Total RNA was isolated from upper and lower petal lobes of 1- to 5-day-old snapdragon flowers by a slightly modified guanidium chloride method, as described by Herdenberger et al. (1990). Poly(A)$^+$ mRNA was isolated from total RNA by using the poly-A-Ttract mRNA Isolation Systems (Promega, Madison, WI). cDNA synthesis was performed according to the cDNA Synthesis Kit (Pharmacia Biotech). A cDNA library was constructed in the Lambda-ZAP II vector (Stratagene, La Jolla, CA) according to the manufacturer's protocol. The titer of the unamplified library was 1.1×10^6.

Isolation and Characterization of cDNA Clones

For polymerase chain reaction (PCR) amplification of fragments of BAMT cDNA, several pairs of degenerate primers were synthesized, based on the peptide sequences. PCR experiments were performed as previously described, using a snapdragon petal–specific cDNA library as the target (Dudareva et al., 1996, 1998a). PCR experiments using the sense 23-mer oligonucleotide 5′-GA(AG)TT(TC)GA(AG)-GT(ACGT)TT(TC)(TC)T(ACGT)AA(TC)GA-3′ for amino acid sequence EFEVFLND (positions 94 to 101 from the N terminus) and the antisense 20-mer 5′-AC(TC)AA(ACGT)CC(TC)TC(ACGT)GC(ACGT)-ACCAT-3′ for amino acid sequence MVAEGLV (positions 237 to 242 from the N terminus) gave a product of 440 nucleotides. The amplified fragment was in turn used to screen the same cDNA library. Several cDNA clones, all containing the same open reading frame, were isolated and sequenced. The sequence of the longest clone was completely determined on both strands. The GenBank accession number of this sequence is AF198492.

RNA Isolation and RNA Gel Blot Analysis

Total RNA samples from floral tissues and petals at different stages of flower development were isolated and analyzed as previously described (Dudareva et al., 1996, 1998a; Wang et al., 1997). A 1.3-kb EcoRI fragment containing the coding region of the *BAMT* gene was used as a probe for RNA gel blot analysis. For determination of tissue-specific expression, 7 μg of total RNA was loaded in each lane; to de-

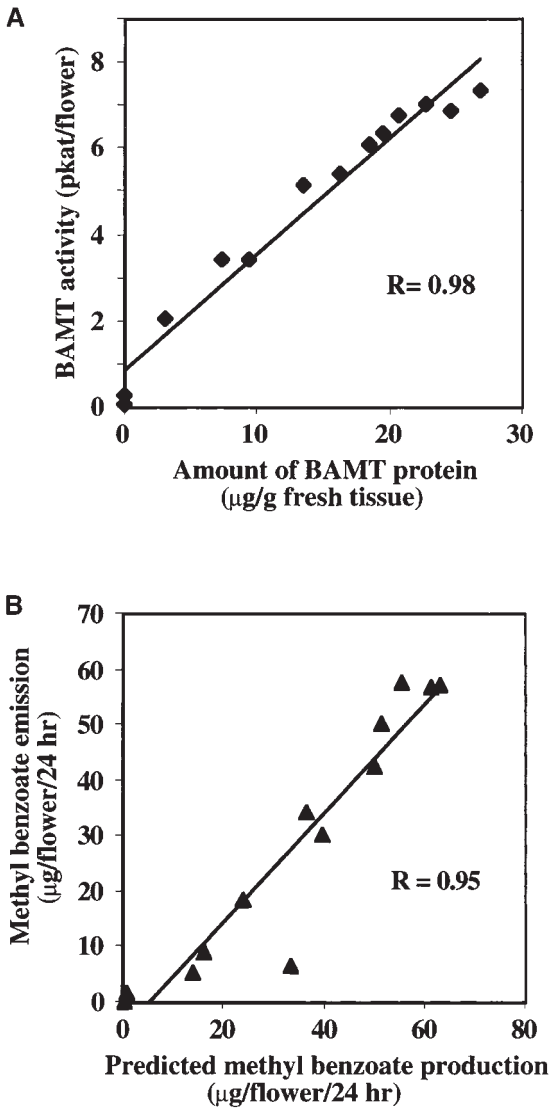

Figure 9. Regulation of Methyl Benzoate Emission in Snapdragon Flowers.

(A) Comparison between BAMT activity and amount of BAMT protein during the life span of the snapdragon flower. BAMT activity data are shown in Figure 3D; the amount of BAMT protein is shown in Figure 7B.
(B) Comparison between emitted amount and predicted production of methyl benzoate during the life span of the snapdragon flower. The emitted amount of methyl benzoate is shown in Figure 1A. The predicted production of methyl benzoate was calculated from Equations 1 and 2 given in Methods.

termine variations in expression over the life span of the flower, 3 μg of total RNA was loaded. Hybridization signals were quantified with a Storm 860 PhosphorImager (Molecular Dynamics, Sunnyvale, CA), and the amounts of *BAMT* mRNA transcripts were normalized to those of rRNA to overcome error in RNA quantitation by spectrophotometry.

Expression of BAMT in *Escherichia coli*

The coding region of BAMT was amplified with the sense 29-mer oligonucleotide 5′-GTCTAGACATATGAAAGTGATGAAGAAAC-3′, which introduced an NdeI site at the initiating ATG codon, and the antisense 29-mer oligonucleotide 5′-TGGATCCTTCATCTCCTACTTAGAGAAAC-3′, which introduced a BamHI site downstream of the stop codon. The PCR-amplified 1.1-kb fragment was cloned into the NdeI-BamHI site of the expression vector pET-T7 (11a) (Novagen, Carlsbad, CA); *E. coli* BL21 (DE3) cells were transformed with recombinant plasmid; and the expression of BAMT cDNA was induced by adding 0.4 mM isopropyl-β-D-thiogalactopyranoside at A_{600} of 0.5 and incubated for 20 hr at 20°C (Yamaguchi et al., 1996). *E. coli* cells were harvested by centrifugation and sonicated, and BAMT activity was measured in the soluble and insoluble fractions.

Extraction of Methyl Benzoate from the Medium of *E. coli* Cells and GC-MS Analysis

BL21 (DE3) cells expressing BAMT and those containing pET-T7 (11a) vector (controls) were grown in the presence (5 μg mL^{-1}) or absence of benzoic acid under the conditions described above. After the cells were harvested by centrifugation, the culture medium (25 mL) was extracted with 5 mL of hexane, the hexane phase was concentrated to 200 μL and analyzed by GC-MS (Dudareva et al., 1998a).

Immunoblots

Crude extracts were prepared from the upper and lower petal lobes of snapdragon flowers at different stages of flower development (from mature buds 1 day before opening on day 12 after anthesis), as described previously (Dudareva et al., 1996). Immunodetection was performed by using rabbit anti–BAMT purified polyclonal antibodies (1:2500 dilution), with goat anti–rabbit IgG horseradish peroxidase conjugate (1:30,000 dilution) as secondary antibody. Antigen bands were visualized using chemiluminescence reagent (New England Nuclear Life Science Products, Boston, MA) for protein gel blots, according to the manufacturer's protocols, and exposing the gels on Eastman Kodak X-OMAT AR film. The results were quantified by densitometry, with use of the Scion (Frederick, MD) Image 1.62c Software package. Preimmune serum was used as a control.

Extraction and Quantification of Endogenous Benzoic Acid

Benzoic acid was extracted from plant tissue by supercritical carbon dioxide extraction at 414 bars and 40°C with an SFX-210 Extractor outfitted with a model 2600 pump and a temperature-controlled variable restrictor (ISCO Inc., Lincoln, NE) (McHugh and Krukonis, 1994). Four grams of petal tissues (upper and lower lobes) at different stages of flower development was extracted with 440 mL of CO_2 at a flow rate of ~7 mL min^{-1}. Extracts were collected into test tubes filled with 4 mL of methanol, filtered through 0.2-μm pore-size nylon filters (Nalgene, Rochester, NY) to eliminate insoluble debris, and concentrated to 150 μL. The samples (25 μL) were injected, and the compounds were separated on a C_{18} reversed-phase HPLC column (Hibar Ec Cartridge containing Merk Lichrosorb RP-18 10-μm C_{18}

reversed-phase packing; 4.6 mm × 25 cm [Alltech Associates, Deerfield, IL]) maintained at 20°C (Graham, 1991). Benzoic acid was separated during a 15-min gradient of methanol (from 25 to 70%) and quantified by UV absorption at 210 nm with a Varian (Walnut Creek, CA) 9050 variable-wavelength UV-VIS detector. Under these conditions, the retention time for benzoic acid was 8.6 min, and the limit of detection was 6 μg mL^{-1} (0.15 μg of benzoic acid per injection). Solutions containing 6 to 120 μg mL^{-1} authentic benzoic acid were used to prepare a standard curve. All data were corrected for benzoic acid recovery, as determined using internally spiked samples.

Benzoic acid in plant extracts was verified by mass spectrometric analysis; its coelution with authentic standard was also confirmed by HPLC. For GC-MS analysis, the benzoic acid peak was collected from the HPLC column and derivatized to a trimethylsilyl ester by adding bis(trimethylsilyl)trifluoroacetamide (Supelco, Bellefonte, PA). The derivatized sample was analyzed with a FinniganMAT GCQ mass spectrometer (Thermoquest). The GC-MS spectrum obtained was compared with that of authentic benzoic acid that had been derivatized in the same way.

Estimation of Predicted Emission of Methyl Benzoate

The predicted production of methyl benzoate was calculated from the Michaelis–Menten Equations 1 and 2.

$$V_{\text{predicted}} = V_{\max}\frac{[S_{\text{BA}}]}{[S_{\text{BA}}] + K_{\text{m}}} \quad (1)$$

where $V_{\max}$ is the maximal rate, $[S_{\text{BA}}]$ is the benzoic acid concentration in petal tissue, K_{m} is Michaelis constant of plant BAMT protein for benzoic acid, which is 1 mM (L.M. Murfitt, N. Kolosova, and N. Dudareva, manuscript in preparation). $[S_{\text{BA}}]$ in petal tissue was calculated from the amount of benzoic acid obtained experimentally (data shown in Figure 8A), assuming that this compound is produced in cytoplasm and that the volume of cytoplasm is 80 μL g^{-1} fresh weight (Winter et al., 1993).

$$V_{\max} = V\frac{(S_{\text{o}} + K_{\text{m}})}{S_{\text{o}}} = \frac{3}{2}V \quad (2)$$

where V is the experimentally obtained activity of BAMT in the upper and lower petal lobes during flower development (data shown in Figure 3D), $[S_{\text{o}}]$ is the concentration of benzoic acid in the enzymatic assays (2 mM in our assay), and K_{m} of plant BAMT protein for benzoic acid is 1 mM.

ACKNOWLEDGMENTS

We thank Dr. Rodney Croteau for his generous gift of *trans*-β-ocimene standard for GC-MS analysis, Nick Rozzi for supercritical extraction of benzoic acid, Iris Heidmann (Max-Planck-Institut für Züchtungsforschung, Cologne, Germany) for her generous gift of pictures of snapdragon flowers with bees, and David Bay for technical assistance with figures. We are also grateful to Dr. David Rhodes for helpful discussions during the preparation of the manuscript. This work is supported by the National Science Foundation (Grant No. IBN-9904910) and by grants from Fred Gloeckner Foundation, Inc. This paper is contribution No. 16183 from Purdue University Agricultural Experimental Station.

Received December 22, 1999; accepted April 4, 2000.

REFERENCES

Bradford, M.M. (1976). A rapid and sensitive method for the quantitation of microgram quantities of protein utilizing the principle of protein–dye binding. Anal. Biochem. **72,** 248–254.

Coen, E.S., and Meyerowitz, E.M. (1991). The war of the whorls: Genetic interactions controlling flower development. Nature **353,** 31–37.

Coen, E.S., Carpenter, R., and Martin, C. (1986). Transposable elements generate novel spatial patterns of gene expression in *Antirrhinum majus*. Cell **47,** 285–296.

Dobson, H.E.M. (1994). Floral volatiles in insect biology. In Insect–Plant Interactions, Vol. 5, E. Bernays, ed (Boca Raton, FL: CRC Press), pp. 47–81.

Dudareva, N., and Pichersky, E. (2000). Biochemical and molecular aspects of floral scents. Plant Physiol. **122,** 627–634.

Dudareva, N., Cseke, L., Blanc, V.M., and Pichersky, E. (1996). Evolution of floral scent in *Clarkia*: Novel patterns of *S*-linalool synthase gene expression in the *C. breweri* flower. Plant Cell **8,** 1137–1148.

Dudareva, N., D'Auria, J.C., Nam, K.H., Raguso, R.A., and Pichersky, E. (1998a). Acetyl CoA:benzyl alcohol acetyltransferase—An enzyme involved in floral scent production in *Clarkia breweri*. Plant J. **14,** 297–304.

Dudareva, N., Raguso, R.A., Wang, J., Ross, J.R., and Pichersky, E. (1998b). Floral scent production in *Clarkia breweri*. III. Enzymatic synthesis and emission of benzenoid esters. Plant Physiol. **116,** 599–604.

Dudareva, N., Piechulla, B., and Pichersky, E. (1999). Biogenesis of floral scent. Hort. Rev. **24,** 31–54.

Graham, T.L. (1991). A rapid, high resolution high performance liquid chromatography profiling procedure for plant and microbial aromatic secondary metabolites. Plant Physiol. **95,** 584–593.

Heidmann, I., Efremova, N., Saedler, H., and Schwarz-Sommer, Z. (1998). A protocol for transformation and regeneration of *Antirrhinum majus*. Plant J. **13,** 723–728.

Heinrich, B. (1979). Bumblebee Economics. (Cambridge, MA: Harvard University Press).

Helsper, J.P.F.G., Davies, J.A., Bouwmeester, H.J., Krol, A.F., and van Kampen, M.H. (1998). Circadian rhythmicity in emission of volatile compounds by flowers of *Rosa hybrida* L. cv. Honesty. Planta **207,** 88–95.

Henderson, A. (1986). A review of pollination studies in the Palmae. Bot. Rev. **52,** 221–259.

Henning, J.A., and Teuber, L.R. (1992). Combined gas chromatography–electroantennogram characterization of alfalfa floral volatiles recognized by honeybees (*Hymenoptera*: *Apidae*). J. Econ. Entomol. **85,** 226–232.

Herdenberger, F., Evrard, J.L., Kuntz, M., Tessier, L.H., Klein, A.L., Steinmetz, A., and Pillay, D.T.N. (1990). Isolation of flower-specific cDNA clones from sunflower (*Helianthus annuus* L.). Plant Sci. **69,** 111–122.

Ibrahim, R.K. (1997). Plant *O*-methyl transferases signatures. Trends Plant Sci. **2,** 249–250.

Ibrahim, R.K., Bruneau, A., and Bantignies, B. (1998). Plant *O*-methyl transferases: Molecular analysis, common signature and classification. Plant Mol. Biol. **36,** 1–10.

Irish, V., and Yamamoto, Y.T. (1995). Conservation of floral homeotic genes function between Arabidopsis and Antirrhinum. Plant Cell **7,** 1635–1644.

Jones, K.N., Reithel, J.S., and Irvin, R.E. (1998). A trade-off between the frequency and duration of bumblebee visits to flowers. Oecologia **117,** 161–168.

Joshi, C.P., and Chiang, V.L. (1998). Conserved sequence motifs in plant *S*-adenosyl-L-methionine–dependent methyl transferases. Plant Mol. Biol. **37,** 663–674.

Knudsen, J.T., and Tollsten, L. (1993). Trends in floral scent chemistry in pollination syndromes: Floral scent composition in moth-pollinated taxa. Bot. J. Linn. Soc. **113,** 263–284.

Knudsen, J.T., Tollsten, L., and Bergstrom, G. (1993). Floral scents—A checklist of volatile compounds isolated by headspace techniques. Phytochemistry **33,** 253–280.

Loughrin, J.H., Hamilton-Kemp, T.R., Andersen, R.A., and Hildebrand, D.F. (1990). Volatiles from flowers of *Nicotiana sylvestris, N. otophora* and *Malus* x *Domestica*: Headspace components and day/night changes in their relative concentrations. Phytochemistry **29,** 2473–2477.

Martin, C., Lister, C., Thijs, H., Prescott, A., Jackson, D., and MacKay, S. (1990). Transposable elements from *Antirrhinum majus*: Their uses in gene isolation and characterization. In Plant Biology, Vol. 11: Horticultural Biotechnology, A.B. Bennett and S.D. O'Neill, eds (New York: Wiley-Liss), pp. 137–153.

Matile, P., and Altenburger, R. (1988). Rhythms of fragrance emission in flowers. Planta **174,** 242–247.

McHugh, M.A., and Krukonis, V.J. (1994). Supercritical Fluid Extraction. (Boston, MA: Butterworth-Heinemann).

Nielsen, J.K., Jakobsen, H.B., Hansen, P.F.K., Moller, J., and Olsen, C.E. (1995). Asynchronous rhythms in the emission of volatiles from *Hesperis matronalis* flowers. Phytochemistry **38,** 847–851.

Oka, N., Ohishi, H., Hatano, T., Hornberger, M., Sakata, K., and Watanabe, N. (1999). Aroma evolution during flower opening in *Rosa damascena* Mill. Z. Natforsch. C Biosci. **54,** 889–895.

Pichersky, E., Raguso, R.A., Lewinsohn, E., and Croteau, R. (1994). Floral scent production in *Clarkia* (Onagraceae). I. Localization and developmental modulation of monoterpene emission and linalool synthase activity. Plant Physiol. **106,** 1533–1540.

Pichersky, E., Lewinsohn, E., and Croteau, R. (1995). Purification and characterization of *S*-linalool synthase, an enzyme involved in the production of floral scent in *Clarkia breweri.* Arch. Biochem. Biophys. **316,** 803–807.

Raguso, R.A., and Light, D.M. (1998). Electroantennogram responses of male *Sphinx perelegans* hawkmoths to floral and "green-leaf" volatiles. Entomol. Exp. Appl. **86,** 287–293.

Raguso, R.A., and Pellmyr, O. (1998). Dynamic headspace analysis of floral volatiles: A comparison of methods. Oikos **81,** 238–254.

Raguso, R.A., and Pichersky, E. (1995). Floral volatiles from *Clarkia breweri* and *C. concinna* (Onagraceae): Recent evolution of floral scent and moth pollination. Plant Syst. Evol. **194,** 55–67.

Raguso, R.A., Light, D.M., and Pichersky, E. (1996). Electroantennogram responses of *Hyles lineata* (Sphingidae: Lepidoptera) to volatile compounds from *Clarkia breweri* (Onagraceae) and other moth-pollinated flowers. J. Chem. Ecol. **22,** 1735–1766.

Ross, J.R., Nam, K.H., D'Auria, J.C., and Pichersky, E. (1999). *S*-adenosyl-L-methionine:salicylic acid carboxyl methyl transferase, an enzyme involved in floral scent production and plant defense, represents a new class of plant methyl transferases. Arch. Biochem. Biophys. **367,** 9–16.

Schiestl, F.P., Ayasse, M., Paulus, H.F., Erdmann, D., and Francke, W. (1997). Variation of floral scent emission and post pollination changes in individual flowers of *Ophrys sphegodes* subsp. *Sphegodes*. J. Chem. Ecol. **23,** 2881–2895.

Sommer, H., and Saedler, H. (1986). Structure of the chalcone synthase gene of *Antirrhinum majus*. Mol. Gen. Genet. **202,** 300–305.

Stubbe, H. (1966). Genetik und Zytologie von *Antirrhinum* L. sect *Antirrhinum*. (Jena, Germany: VEB Gustav Fisher Verlag).

Von Frisch, K. (1971). Bees: Their Vision, Chemical Senses, and Language. (Ithaca, NY: Cornell University Press).

Wang, J., and Pichersky, E. (1998). Characterization of *S*-adenosyl-L-methionine:(iso)eugenol *O*-methyl transferase involved in floral scent production in *Clarkia breweri*. Arch. Biochem. Biophys. **349,** 153–160.

Wang, J., Dudareva, N., Bhakta, S., Raguso, R.A., and Pichersky, E. (1997). Floral scent production in *Clarkia breweri* (Onagraceae). II. Localization and developmental modulation of the enzyme *S*-adenosyl-L-methionine:(iso)eugenol *O*-methyl transferase and phenylpropanoid emission. Plant Physiol. **114,** 213–221.

Winter, H., Robinson, D.G., and Heldt, H.W. (1993). Subcellular volumes and metabolite concentrations in barley leaves. Planta **191,** 180–190.

Yamaguchi, S., Saito, T., Abe, H., Yamane, H., Murofushi, N., and Kamiya, Y. (1996). Molecular cloning and characterization of a cDNA encoding the gibberellin biosynthetic enzyme *ent*-kaurene synthase B from pumpkin (*Cucurbita maxima* L.). Plant J. **10,** 203–213.

Developmental Regulation of Methyl Benzoate Biosynthesis and Emission in Snapdragon Flowers
Natalia Dudareva, Lisa M. Murfitt, Craig J. Mann, Nina Gorenstein, Natalia Kolosova, Christine M. Kish, Connie Bonham and Karl Wood
Plant Cell 2000;12;949-961
DOI 10.1105/tpc.12.6.949

This information is current as of March 4, 2021

References	This article cites 36 articles, 7 of which can be accessed free at: /content/12/6/949.full.html#ref-list-1
Permissions	https://www.copyright.com/ccc/openurl.do?sid=pd_hw1532298X&issn=1532298X&WT.mc_id=pd_hw1532298X
eTOCs	Sign up for eTOCs at: http://www.plantcell.org/cgi/alerts/ctmain
CiteTrack Alerts	Sign up for CiteTrack Alerts at: http://www.plantcell.org/cgi/alerts/ctmain
Subscription Information	Subscription Information for *The Plant Cell* and *Plant Physiology* is available at: http://www.aspb.org/publications/subscriptions.cfm

© American Society of Plant Biologists
ADVANCING THE SCIENCE OF PLANT BIOLOGY